Population equations for degree-heterogenous neural networks

M. Kähne, I. M. Sokolov, and S. Rüdiger
Institut für Physik, Humboldt-Universität zu Berlin, Germany
(Received 30 May 2017; revised manuscript received 4 August 2017; published 6 November 2017)

We develop a statistical framework for studying recurrent networks with broad distributions of the number of synaptic links per neuron. We treat each group of neurons with equal input degree as one population and derive a system of equations determining the population-averaged firing rates. The derivation rests on an assumption of a large number of neurons and, additionally, an assumption of a large number of synapses per neuron. For the case of binary neurons, analytical solutions can be constructed, which correspond to steps in the activity versus degree space. We apply this theory to networks with degree-correlated topology and show that complex, multi-stable regimes can result for increasing correlations. Our work is motivated by the recent finding of subnetworks of highly active neurons and the fact that these neurons tend to be connected to each other with higher probability.

DOI: 10.1103/PhysRevE.96.052306

I. INTRODUCTION

The information processing by large ensembles of neurons has often been discussed in the context of population coding. This refers to the assumption that no single neurons are responsible for the computational processes in the brain, but rather populations of neurons [1,2]. Accordingly, in this approach, firing rates of individual neurons are averaged over the entire population and the information from the heterogeneity of firing rates is discarded. However, there is increasing evidence that in many brain structures subnetworks of highly active neurons exist. Yassin *et al.* have shown that a large fraction of neurons in the neocortex fire at extremely small rates, while a small fraction of neurons are highly active [3]. Furthermore, they have observed that the highly active neurons are linked to each other with a higher probability. Nigam *et al.* estimated that 70% of the information is transmitted through only 20% of the neurons forming a hub, or a rich club [4].

Population coding is known to be the underlying principle for a variety of sensory functioning in the brain [5–8] and has often been discussed mathematically, for instance, in terms of information content and tuning curves [9,10], or in relation to direction sensory functioning [11]. Population equations or neural field models are a fruitful mathematical approach to neural information processing.

The additional heterogeneity of neurons in the population has also been incorporated, mostly regarding the different types of neurons (e.g., excitatory versus inhibitory) as well as spatial distribution of neurons [12,13]. However, the statistical heterogeneity in degree, as described in the recent experiments, has rarely been discussed so far. Here we try to close this gap by introducing a distribution of the neuron's degree as well as correlations in degrees of interacting neurons.

Our discussion will be based on the investigation of systems of equation for firing rates on neurons. Concentrating on the firing rate (which we will also refer to as activity) and not on precise temporal evolution of each neurons membrane potential, has a long history in neuroscience starting with Ref. [14] where it was first demonstrated that it is this rate which governs the information transmission in interneuronal communication, a phenomenon that is now commonly discussed within the context of rate coding.

We first show that averaging of the firing-rate equations over neurons of same degree can lead to a well-defined system of equations for the averaged firing rates. This result hinges on the fact that in neural ensembles both the number of neurons as well as the *number of synapses per neuron* is typically large. We argue that in this case one can interchange the averaging over neurons with the application of the firing rate function, which leads to a drastically reduced system of equations corresponding to a mean-field approximation.

In certain cases, e.g., when the firing rate function is binary, analytical solutions of these population equations can be constructed. Indeed, it is straightforward to find solutions with highly connected active subpopulations. Moreover, we show that one can study the behavior of the neuronal system under increasing levels of degree correlation in the network, which can lead to a transition to multistable solutions for the activity. The comparison of the results of direct simulation of the neuronal system of tens of thousands neurons with the ones of our reduced description shows that the last performs extremely well in a large domain of parameters and gives theoretical explanation of what is seen in such numerical simulations.

There are different approaches to formally introduce or to control correlations in complex networks [15,16]. Within this work we follow a previous study in which the influence of the topology of a network of spiking neurons on the response to a stimulus was studied [10]. Therein correlations are described in terms of conditional probabilities. Especially for directed networks, this proves to be a handy way to explore the connection between the structure of a network and its functional properties.

II. MATHEMATICAL ANALYSIS OF COUPLED POPULATION EQUATIONS

We consider a neural network with recurrent connectivity. The firing rate of each individual neuron is given by v_i, where i, $1 \leqslant i \leqslant N$, denotes the neuron's number. Those systems have often been modeled by equations of the form

$$\tau \frac{\partial v_i}{\partial t} = -v_i + f_{\text{recurrent},i}, \tag{1}$$

where τ is a time constant that describes the time scale on which the firing rate relaxes toward its steady-state value. On a microscopic level, i.e., considering every single neuron i within the network, the synaptic input current depends on the properties of the synapses within the network. The function f is usually referred to as activation or transfer function. The dimension of the firing rate, and therefore of the transfer function f, is the one of the frequency, i.e., of the inverse time.

In this work we are solely interested in the influence of the networks topology on the network's self-sustained activity and therefore consider all synapses to be identical of unit coupling strength. Also no synaptic time delays or external input is considered. The recurrent input to neuron i can then be written as $f_{\text{recurrent},i} = f(\sum_j a_{ji} v_j)$, with a_{ji} being the entries of the adjacency matrix of the network, which are unity if there is a link from node j to node i, and zero otherwise. The transfer function f is often assumed to have a sigmoidal form. The firing rate of any realistic neuron model is bounded from above. Normalizing v_i over the maximal firing rate we get the dimensionless form of the corresponding Eq. (1). Such a dimensionless rate will be often called the neuron's activity in what follows. This variable is bounded to a unit interval. We will also assume that the domain of values of f is also $[0,1]$.

Following the previous work [10], we consider directed networks, in which each neuron has an equal number of incoming and outgoing synapses. This in- and out-degree will be denoted by k and is distributed according to the probability distribution $P(k)$. The set of all neurons of degree k in the network is called k-population. For ease of computation we will usually assume that the distribution $P(k)$ has cutoffs at small and large k, i.e., is concentrated on the interval between $k_{\min}$ and $k_{\max}$.

A. Population approach

One main goal of our work is to derive and discuss equations for population activities u_k of a k population defined as

$$u_k = \frac{1}{N_k} \sum_{i=1}^{N} v_i \delta_{k_i,k} = \frac{1}{N_k} \sum_{i:k_i=k} v_i, \tag{2}$$

where $N_k = \sum_{i=1}^{N} \delta_{k_i,k} \simeq N P(k)$ is the number of neurons in the k population. The network's heterogeneity is characterized in terms of the average number $N(k,k')$ of direct links from the k' population to the k population: For every input link of a k neuron the probability that this link originates in a k' neuron is $N(k,k')/k$.

Mapping the dynamics from the neural network equations Eq. (1) to the population firing rates Eq. (2) requires two steps:

(1) As is usually the case in population models, we assume that the firing rates of a k neuron can be approximated by the mean firing rates of the entire k population, $v_i \approx \langle v_i \rangle \equiv u_k$ for all neurons i whose degree k_i is equal to k. It means that the only relevant property of a neuron, determining the heterogeneity of the neurons in the population, is the input degree. If, for instance, two neurons in the k population have sets of input neurons with different degrees, their firing rates will be statistically the same. This is a strong, although intuitive assumption. Below, using analytical as well as numerical considerations, we will show that this procedure generates useful generalization of the standard population approach, where one puts all neurons into a single population.

(2) Combining Eqs. (1) and (2) allows us to obtain an equation for the population average u_k, which reads

$$\tau \frac{\partial u_k}{\partial t} = -u_k + \frac{1}{N_k} \sum_{i:k_i=k} f\left(\sum_j a_{ji} v_j \right), \tag{3}$$

with $k_{\min} \leqslant k \leqslant k_{\max}$. The second term on the right-hand side represents the steady-state firing-rate averaged over all k neurons. However, to obtain a closed system of equations for u_k it needs to be rewritten in terms of the weighted average of mean firing rates $u_{k'}$. Since this involves interchanging the averaging with the application of a nonlinear function this is not necessarily possible.

Under certain conditions, however, this second step can be performed and, as shown in Appendix A 1, we obtain

$$\tau \frac{\partial u_k}{\partial t} = -u_k + f\left(\sum_{k'} N(k,k') u_{k'} \right). \tag{4}$$

It should be noted that we here rely on the fact that, in addition to a large number of neurons in the population, the number of synapses per neuron is sufficiently large, so that the quantity $\sum_j a_{ji} v_j$ hardly fluctuates. Equation (4) represents the mean-field approximation to Eq. (3), and the numerical simulations of the full system show that these equations perform very well and lead to important insights.

Note that Eqs. (1)–(4) describe the general case of continuous-time evolution of neuronal activities for general transfer functions f. For most of this work, we will, however, limit ourselves to discrete-time systems, where the differential equations reduce to a map and take f to be a Heaviside step function. This fixes the possible activity states of the neurons to 0 or 1. The situation is thus described by a binary neuron model, sometimes referred to as McCulloch-Pitts model [17], for which we report our most important findings. We will, however, turn back to the continuous-time evolution of population activities and to more general transfer functions in Appendix B when discussing the generality of the approach proposed.

B. Network correlations

In the following, we will briefly introduce common concepts to describe correlations in networks to achieve a better understanding of the joint distribution function $N(k,k')$. Correlation in networks usually refers to the correlation between degrees of pairs of connected nodes. For quantifying purposes it is useful to introduce an edge end distribution, which is the degree distribution at one end of a randomly selected edge. It reads $P_e(k) = kP(k)/\langle k \rangle$, [15,18], where $\langle k \rangle$ is the mean degree of the network with respect to nodes, $\langle k \rangle = \sum_k kP(k)$. Correspondingly, one can define a joint probability distribution $P(k,k')$ giving the probability that a randomly chosen link connects nodes with degrees k and

k'. For uncorrelated networks this is $P_{\rm unc}(k,k') = P_e(k)P_e(k')$. The correlations are then formally introduced via

$$P(k,k') = P_e(k)P_e(k')g(k,k'), \tag{5}$$

as in Ref. [15]. It is then natural to define a conditional probability

$$P(k|k') = P(k,k')/P_e(k') = P_e(k)g(k,k'), \tag{6}$$

which is the probability to find a node of degree k, when following a link that originates from a node of degree k'. As in previous work [10], we treat heterogeneity in networks by employing the joint distribution function $N(k,k')$, which is defined as

$$N(k,k') = kP(k'|k). \tag{7}$$

For a given network realization, this corresponds to the number of links that point from k' neurons to k neurons, averaged over all k neurons. For uncorrelated networks, the joint distribution function reads

$$N(k,k') = \frac{kk'P(k')}{\langle k\rangle} = N(k,k')^{\rm unc}. \tag{8}$$

It is useful to list the properties of the joint distribution function that follow the above definitions:

$$N(k,k') \geqslant 0, \quad \forall\, k,k', \tag{9}$$

$$\sum_{k'} N(k,k') = k, \tag{10}$$

$$\sum_{k} P(k)N(k,k') = k'P(k'), \tag{11}$$

which are discussed in Appendix A 2 in more detail. While Eq. (8) defines uncorrelated networks, in principle any joint distribution function that obeys conditions Eqs. (9)–(11) represents an ensemble of networks. To obtain one realization of this ensemble of networks, also the number N of the neurons, and the degree distribution $P(k)$ are required, as the joint distribution function $N(k,k')$ only constraints the wiring possibilities. The constraints on the joint distribution function, given by Eqs. (9)–(11), allow the formal introduction of degree correlations of the form

$$N(k,k') = N(k,k')^{\rm unc} + \gamma\frac{\eta(k,k')}{P(k)}, \tag{12}$$

with

$$\sum_{k} \eta(k,k') = \sum_{k'} \eta(k,k') = 0. \tag{13}$$

The function $\eta(k,k')$ describes the deviation from the uncorrelated network and γ is a parameter describing the strength of this deviation. The values of γ are constrained by the positivity of the joint distribution function, Eq. (9); see Appendix A 3 for more detail. For the remaining part of this work, we focus on one possible choice of η that fulfills Eq. (13), i.e.,

$$\eta(k,k') = (k-k_0)(k'-k_0), \tag{14}$$

where $k_0 = (k_{\rm max}+k_{\rm min})/2$, so that the resulting joint distribution function reads

$$N(k,k') = \frac{kk'P(k)}{\langle k\rangle} + \gamma\frac{(k-k_0)(k'-k_0)}{P(k)}. \tag{15}$$

Using this simple choice for $\eta(k,k')$ we will illustrate how nontrivial mixing can be introduced into complex networks, and what are the effects of such mixing on the firing rates.

C. Steady-state solutions for Heaviside step functions

In the following, we want to find steady-state solutions for the population activities u_k in the system Eq. (4). Generally, this requires knowledge about the specific form of the recurrent activation function f. One often assumes a sigmoidal relation, and approximates $f(u)$ by $f(u) \approx 1/[1+\exp(-u)]$, or alternatively $f(u) \approx 1+\mathrm{erf}(u)$ [19]. To discuss stationary solutions for the population activity, we will approximate this sigmoidal function by a step, i.e., by a Heaviside θ-function: $f(u) \sim \theta(u-\Theta)$. Consequently, for the stationary case and under the population-dynamic assumption, Eq. (4) reduces to

$$u_k = \theta\left(\sum_{k'} N(k,k')u_{k'} - \Theta\right). \tag{16}$$

The threshold Θ is a property of the neurons. For example, in the case of spiking neurons modeled by some sort of integrate and fire system, it translates to the membrane potential threshold, which, if exceeded, leads to a spike of the neuron. Similarly, the population activity can be interpreted as an order parameter $u_k \in [0,1]$, which is 1 (0) if the population is active (inactive). Then the threshold Θ represents the critical number of input links from active neurons. Equation (16) corresponds to a system known as McCulloch-Pitts model [17] and has, e.g., been discussed in the context of memory capacity of a neuronal network [20]. Note that the system of equations for the population activity [Eq. (16)] itself can be interpreted as a recurrent neuronal network with u_k describing the state of neuron k and $N(k,k')$ being the interaction matrix between neuron k and k'. Equation (16) reduces to

$$u_k = \begin{cases} 1, & \text{if } \sum_{k'} N(k,k')u_{k'} \geqslant \Theta \\ 0, & \text{otherwise.} \end{cases} \tag{17}$$

Now we seek self-consistent solutions of this last expression. Clearly, $u_k = 0$ for all k is always a solution provided that $\Theta > 0$. However, there may be further solutions in which u_k is k-dependent. The simplest case of such solutions is a step solution at some threshold degree κ between $k_{\rm min}$ and $k_{\rm max}$:

$$u_k = \begin{cases} 1, & \text{if } k \geqslant \kappa, \\ 0, & \text{otherwise.} \end{cases} \tag{18}$$

Note that since large-k neurons have more input links than small-k neurons, the former will be more likely to be active than the latter and thus the step solution seems natural. In that case the summation in Eq. (16) simplifies to

$$u_k = \theta\left(\sum_{k'=\kappa}^{k_{\rm max}} N(k,k') - \Theta\right), \tag{19}$$

and therefore Eq. (18) satisfies Eq. (17) if

$$\sum_{k'=\kappa}^{k_{\rm max}} N(\kappa,k') \geqslant \Theta \quad \text{and} \quad \sum_{k'=\kappa}^{k_{\rm max}} N(\kappa-1,k') < \Theta. \tag{20}$$

For simplicity we seek κ with

$$\sum_{k'=\kappa}^{k_{\max}} N(\kappa,k') = \Theta. \tag{21}$$

The remainder of the sum is only a function of κ and we will therefore refer to it as

$$F(\kappa) = \sum_{k'=\kappa}^{k_{\max}} N(\kappa,k'), \tag{22}$$

and thus we find the condition

$$0 = F(\kappa) - \Theta \tag{23}$$

for step steady-state solutions of the system.

D. Example

An analytical approach to our problem requires the calculation of the sum in Eq. (21). One specific choice that allows for an exact calculation are networks with a flat degree distribution within a given range of degrees given by

$$P(k) = \begin{cases} C, & k \in [k_{\min}, k_{\max}] \\ 0, & \text{otherwise}, \end{cases} \tag{24}$$

with $C = 1/(k_{\max} + 1 - k_{\min})$. The joint distribution function is then given by

$$N(k,k') = \frac{kk'C}{k_0} + \gamma \frac{(k-k_0)(k'-k_0)}{C}, \tag{25}$$

where again we used the constant $k_0 = (k_{\max} + k_{\min})/2$. Requiring $N(k,k')$ to be positive limits the correlation strength parameter to

$$\gamma \in \left[-\frac{4k_{\min}C^2}{k_0 \Delta k^2}, \frac{4k_{\min}k_{\max}C^2}{k_0 \Delta k^2} \right], \tag{26}$$

where $\Delta k = k_{\max} - k_{\min}$. Figure 1 shows the joint distribution function for uncorrelated networks in the k,k' plane in blue. The red mash shows the maximally correlated case $\gamma = \gamma_{\max} \approx 1.45 \times 10^{-6}$ for the range of degrees of this example, i.e., $k \in [100,240]$. One can see that the correlation between the population of minimal degree (here $k = 100$) and itself is increased compared to the uncorrelated case, which is also true for the population of maximal degree (here $k = 240$). On the contrary, the correlation between the population of maximum degree and the population of minimum degree is reduced, compared to the uncorrelated case. For our particular choice of correlation, this is the limiting point for the strength parameter γ, as choosing any higher value would lead to negative values, which are prohibited by Eq. (9). Analogously, for negative strength parameters, there is a lower bound. In that case the "self-correlation" of the smallest population degree is the first to approach zero, while the correlation between the smallest and the highest population is larger compared to the uncorrelated case. (This case does not lead to more interesting dynamics and is therefore not displayed in the plot Fig. 1.)

For uncorrelated networks with a flat degree distribution, as defined by combining Eqs. (8) and (24), Eq. (22) leads to

$$F(\kappa) = \sum_{k'=\kappa} N(\kappa,k') = \frac{C\kappa}{k_0} \sum_{k'=\kappa}^{k_{\max}} k' \tag{27}$$

$$= \frac{C\kappa}{2k_0}[k_{\max}(k_{\max}+1) - \kappa(\kappa-1)]. \tag{28}$$

Thus, according to Eq. (23), we expect stationary solutions for κ if

$$0 = \frac{C\kappa}{2k_0}[k_{\max}(k_{\max}+1) - \kappa(\kappa-1)] - \Theta. \tag{29}$$

The expression above is a polynomial of third order in κ, which allows for up to three real solutions. These solutions can be understood such that for a given threshold Θ, there are possibly three values for $\kappa = \kappa_{1,2,3}$ above and including which degree, all populations are active, so $u_k = 1, \quad \forall \quad k \geqslant \kappa$. In Fig. 2(a) we show the function $F(\kappa)$ for a number of different threshold values Θ and in Fig. 2(b) we show self-consistent solution for Eq. (21) for the uncorrelated network with flat degree distribution.

The blue dashed line in Figs. 2(a) and 2(b) illustrates an exemplar threshold, i.e., the number of input links from active neighbors, that is required for a neuron to be active. The black

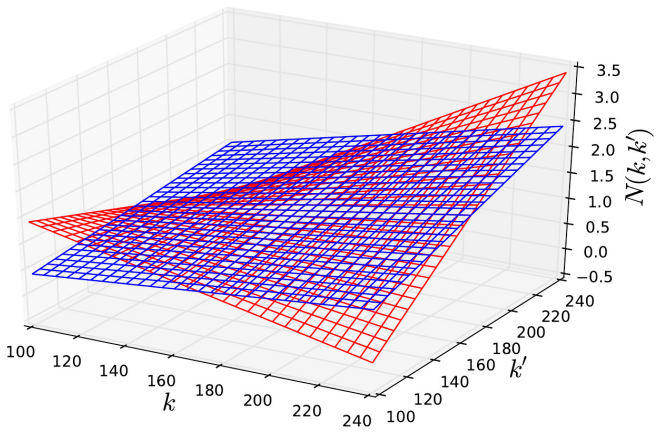

FIG. 1. The joint distribution function $N(k,k')$ for $k,k' \in [100,240]$ for the maximal possible correlation strength parameter γ (red) and the joint distribution function $N(k,k')^{\text{unc}}$ (blue) for the same degree range.

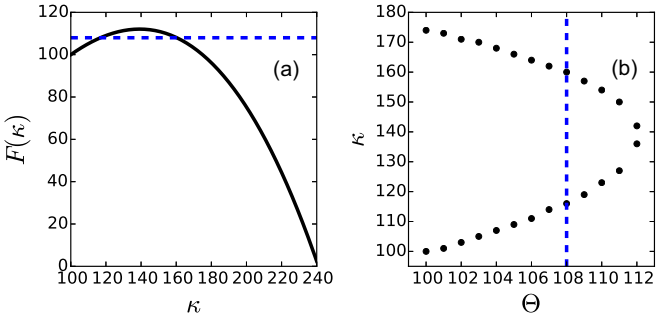

FIG. 2. (a) The function $F(\kappa)$ vs. κ for a network with a flat degree distribution with $100 \leqslant k \leqslant 240$. The blue dashed line indicates an exemplary threshold, in this case $\Theta = 108$. Intersections of $F(\kappa)$ and this threshold give the solutions of the self consistent equation $0 = F(\kappa) - \Theta$, which are shown in (b) for a number of different thresholds.

dots in Fig. 2(b) represent the solutions of Eq. (23) for κ. As can be seen $F(\kappa = k_{\min}) = k_{\min}$, which is consistent with what is expected from Eq. (10). In other words, setting the threshold value Θ equal to the minimum possible population degree $k_{\min}$ yields one solution at $\kappa = k_{\min}$, thus a completely active network. This is quite intuitive, because $\Theta = k_{\min}$ does not forbid any population to be active by default.

III. METHODS

In this section, we briefly discuss the methods that were used for a numerical validation of the theory. Namely, we describe the algorithm used to create realizations of the ensemble of networks with given number of neurons N, degree distribution $P(k)$, and joint distribution function $N(k,k')$.

A. Methods—Network creation

The creation of a network realization of the ensemble of networks defined by $\{N, P(k), N(k,k')\}$ foots on one basic idea. "Measuring" the joint distribution function from a given network boils down to the calculation of histograms of the degrees of all neurons that are connected to all neurons of the same degree, i.e., to one entire population. Inversely, we can generate a realization of a network with a desired joint distribution function by assigning outgoing links from all neurons of one population in a way that the expected histogram is met. Specifically, a histogram of the degree of all neurons that have incoming links from neurons of degree k must approach $NP(k)N(k,k')$. The reason for this is that $NP(k)$ is roughly the number of neurons with degree k, and $N(k,k')$ is roughly the average number of links that point from a neuron of degree k to a neuron of degree k'. Note that in our example N and $P(k)$ are constant, and thus the histogram corresponds to a cut through the surface shown in Fig. 1 along the line corresponding to a chosen degree k'.

Thus, since we know what histogram should be created, we randomly select as many neurons (with open stubs) as required and put them all into one list. Note that this list contains $kN_k = \sum_{k'} N_{k'} N(k,k')$ indices of neurons, consistent with Eq. (11). Then we take all neurons of degree k and connect each to k randomly selected neurons of this list. This is repeated subsequently for all populations of the network, until there is no neuron left with open stubs, i.e., the network is completely connected. Note that at the point when neuron indices are added to a list that holds all available neurons, every neuron of degree k is added to the list the number of times, which is equal to k minus the number of its already assigned in-neighbors, i.e., it is added once for its every open in-pointing stub. Then links are assigned to randomly chosen neurons from that list of indices. The algorithm obviously doesn't avoid double or self links (which is sometimes desirable but not generally required). A multiple link between the two neurons may be interpreted as a single link with higher synaptic coupling strength, i.e., may be considered to mimic the situation where not all synapses are assumed to have equal properties.

Note that even though double and self links are allowed, not every joint distribution function is perfectly realizable. This has mainly two reasons. First, the actual distribution of degrees can, but must not, be perfectly equivalent to the desired degree distribution. Second, the joint distribution function is a matrix whose entries are real rather than natural numbers, as it would be required to assign a perfectly matching number of links. Therefore, its entries are rounded of to the corresponding integer part, whenever the number of links between two populations is calculated.

B. Methods—Binary neurons

To demonstrate the correctness of the calculated steady-state solutions, we discuss simulation results of the spreading of simple time-discrete binary, or two-state neurons, sometimes referred to as McCulloch-Pitts neurons [17]. These are fully characterized by being in one of the two possible states which we will refer to as the active and the passive one. The state v_i of the neuron i depends on the number of input links from other active neurons. If this number exceeds a certain threshold Θ in one time-step, the neuron is active in the next, independently of the current state of the neuron. In one iteration of such a discrete-time procedure, the numbers of all active neighbors are counted for all neurons in the current state. Then the state of the system updated according to

$$v_i(t+1) = \theta\left(\sum_j a_{ij} v_j(t) - \Theta\right); \tag{30}$$

see Chapter 12.2.1 of Ref. [19]. This system is known to be able to show bistability under appropriate conditions (see, e.g., Refs. [21,22]). In Appendix B we will briefly discuss the temporal evolution of such a system as described by the population equations Eq. (4) in continuous time, as well as different degree distributions and transfer functions. The continuous-time representation is also more convenient for performing the stability analysis of the solutions as discussed in Sec. V A.

IV. RESULTS

A. Steady-state firing in uncorrelated networks with flat degree distribution

For the simulation, we created networks with $N = 80\,000$ neurons. As shown below, the steady-state activity depends on the initial conditions of the system. In our simulations we use the initial condition where all neurons with degree larger then a given threshold k_{init} are initialized in the active state. Then we let the system evolve and wait until it reaches the steady state. This is registered when all neurons do not change their state during two consecutive iteration steps. Figure 3 shows the convergence behavior for an uncorrelated network for different numbers of initially active neurons in the system with $\Theta = 108$. The figure shows that there are two possible steady states to which the activity pattern converges. One of them is a trivial one with no active neurons at all, another one has a nonzero number of active neurons. These two represent stable fixed points of the system's dynamics. The nontrivial stable point is labeled as I in Fig. 3. One can also see that there is a clear line above and below which the system strives to one of the steady-state regimes, indicating the existence of the unstable fixed point labeled as II in Fig. 3. The evolution of the three specific initial conditions is indicated by the green,

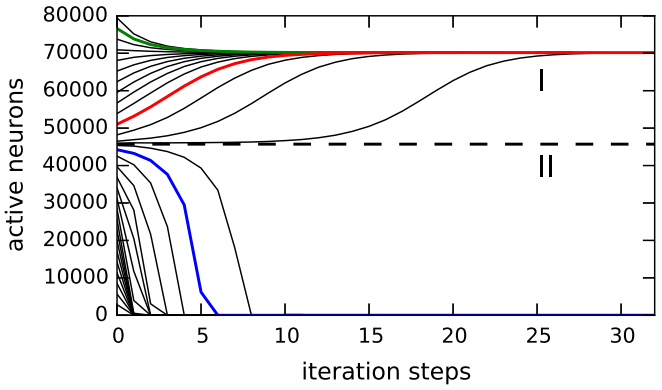

FIG. 3. The number of active neurons versus the number of iteration steps. Different lines correspond to simulations with different initial conditions. This image captures the convergence behavior of an uncorrelated network of $N = 80\,000$ binary neurons with a threshold of $\Theta = 108$, whose degree is flatly distributed in a range of $k \in [100,240]$.

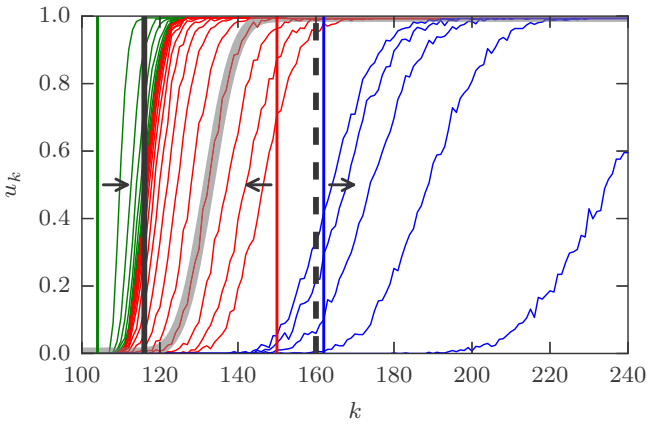

FIG. 4. The time evolution of the population activity for the three exemplary initial conditions discussed in Fig. 3. Every line corresponds to the population activity after one subsequent iteration step starting with the initial conditions indicated by the vertical lines of the same color. The expected stable and unstable stationary solutions shown in Fig. 3 are displayed as solid and dashed black lines. Starting from the initial step function, the shape of the curve rapidly changes to a sigmoidal "front," which retains its form while traveling along the κ axis.

red, and blue lines. Figure 3 suggests that the system under investigation possesses exactly one nontrivial stable and one unstable fixed point.

The specific degree that corresponds to the unstable fixed point II in Fig. 3 will be denoted by κ_u and is simply determined as the number of neurons per population, N_k, times the number of populations, starting from the largest, that would have to be active to achieve the equivalent number of active neurons indicated by the dashed black line II in Fig. 3. The number of active neurons in the system is given by

$$N_{\text{active}} = N \sum_{k=k_{\min}}^{k_{\max}} P(k) u_k = N \sum_{k=\kappa}^{k_{\max}} C \tag{31}$$

$$= NC(k_{\max} - \kappa + 1), \tag{32}$$

where C is the normalization constant in Eq. (24). Thus, because N_k and $k_{\max}$ are fixed, and N_{active} can be observed from the simulation, we can use Eq. (32) to calculate κ_u.

Figure 3 shows that relaxation of the system to its steady state takes only a few iteration steps, i.e., happens very fast. We note that the initial number of active neurons can be interpreted as a stimulus to the system, and the number of active neurons in the steady state as the corresponding response. Then, the rather fast relaxation of the system corresponds to a rapid information transfer through the system. The dependence of the response time on the system's size is weak due to the small-world topology of all networks considered in this work and also of realistic subnetworks of neurons in the brain. The only case in which we observed slightly prolonged relaxation times in our simulations was when the threshold value Θ was chosen close to but below the bifurcation point, and for the network sizes small enough. In this case we observed the system to "almost" converge to the steady-state solution but then eventually turn to an inactive state, as illustrated in Fig. 9. This is a finite-size effect that will be discussed in detail in Sec. V.

Figure 4 shows the time evolution of the population activity "fronts" in time. It can be seen that during the temporal evolution, the shape of the front remains very similar, while it propagates toward a stable fixed point. For initial conditions past the unstable population degree (shown with blue lines), the front vanishes, i.e., converges to the trivial stable fixed point of a completely inactive network. For initial conditions below the unstable population degree (red and green lines), the "fronts" move toward the nontrivial stable solution, which is marked by I in Fig. 4. The gray line in Fig. 4 shows a fit of the population activity after the fourth iteration to an error function. It can be seen that the resulting population activity is very well approximated by an error function. From the population activity in the nontrivial steady state (indicated as I in Fig. 3) we define the position κ_s of the stable steady state solution as the population degree κ at which $u_\kappa(1 - u_\kappa)$ attains its maximum. This turned out to be a very robust method for approximating κ_s in the sense that even though the particular values of the population activities u_k varied in different network realizations, no changes in the estimated values of κ_s were ever observed for networks of $N = 80\,000$ neurons.

In Fig. 5(a) we show the steady-state population activity u_k against the population degree k for a number of different threshold values Θ. From left to right, the lines correspond to increasing thresholds Θ. We find that for smaller threshold values, approximating the population activity as step function is quite good, for larger values of Θ, the sigmoid function u_k appears less steep. Our findings show that the population activity u_k monotonically increases with k, which agrees well with the intuitively assumed functional dependance.

Figure 5(b) shows the approximated steady state population degree κ_∞ as function of the initial population degree κ_0 that was set at the beginning of the simulation for the same values of Θ as in a. It can accordingly be seen as a tuning curve, showing the response of the system (κ_∞) as function of the stimulus (κ_0). All curves show the same characteristic behavior: $\kappa_\infty \geqslant k_{\min}$

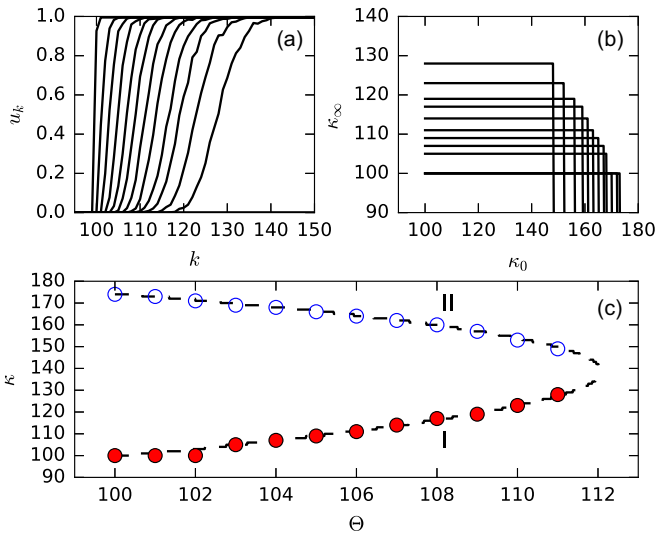

FIG. 5. The figure above shows the simulation results for an uncorrelated network of $N = 80\,000$ neurons with flat degree distribution. The simulations were carried out for threshold values $\Theta \in [100,111]$. (a) The population activity u_k against the population degree k. Every line corresponds to the population activity, after the dynamics died out within the network, i.e., further iterations did not lead to a changed state of any neuron. Lines from left to right correspond to simulations with increased threshold value. (b) The calculated steady-state solution degree κ_∞ as function of the population degree κ_0, above and including which all neurons were initially active in the simulation. Therein, vertical lines from left to right correspond to simulations with decreasing threshold value. (c) The stable (red dots on the lower branch) and unstable (blue hollow dots on the upper branch of the curve) fixed points calculated from simulations (see text for details) as functions of the threshold Θ. The dashed line corresponds to solutions of the equation $F(\kappa) - \Theta = 0$; cf. Fig. 2.

stays constant up to a certain point at which they jump to zero (which is not seen from the plot cut at its lower part). This point corresponds to the unstable fixed point κ_u, while the nonzero constant value represents nontrivial stable fixed point κ_s and zero corresponds to the trivial stable one.

In Fig. 5(c) we plot κ_u (blue circles) and κ_s (red circles) for a number of different threshold values against the values of κ, which solve Eq. (21) and were shown in Fig. 2. It can be seen that the values agree very well for the entire range of chosen thresholds, ranging from the minimal degree $k_{\min} = 100$ to the largest value allowing for the solution of $F(\kappa) - \Theta = 0$ (Fig. 2), i.e., $\Theta = 112$ for this specific system. The surprisingly good agreement justifies the approximation of the population activity by a Heaviside step function. Even for larger threshold values Θ, where the steady-state population activity shows a broad range of populations that are not completely active nor completely inactive, the approximate solution agrees very well with the numerical one.

The roman numerals shown in Fig. 5 mark the stable and unstable branches of the solutions (cf. Figs. 3 and 4): The lower branch I in Fig. 5 is the stable solution and the upper branch II in Fig. 5 is the unstable one. Note that a higher initial degree κ corresponds to a smaller number of initially active neurons. The same roman numerals are used in Fig. 3 to show the corresponding state, but in that case only for the threshold $\Theta = 108$.

Let us summarize the findings of this section with respect to the analytical approximation used. We have a system of equations of the following form:

$$u_k = \theta[F(\kappa) - \Theta]. \tag{33}$$

For the current system (flat degree distribution, no degree-correlations), there are two solutions for the population degree $k = \kappa_{1,2}$ that correspond to vanishing of the argument of the Heaviside step function:

$$F(\kappa_{1,2}) = \Theta. \tag{34}$$

The numerical simulations suggest these indeed indicate the regime change and that one of these solutions corresponds to the stable and another one to the unstable fixed point of the dynamics. We referred to them as κ_u and κ_s. It is rather difficult to give a mathematically rigorous discussion of the stability properties of the steady-state solutions of our system with discontinuous dependencies; Sec. V A, however, gives hints on the reasons for the observed behavior.

B. Steady-state firing in correlated networks with flat degree distribution

The example discussed above shows the existence of three steady-state solutions: two stable solutions, where one is a zero-activity state and the other is a step solution, and one unstable step solution. In correlated networks, we may encounter more complex situations. This is demonstrated by the case for $k \in [100,240]$ as shown in Fig. 6. In this figure we plotted the function $F(\kappa)$ as defined by Eq. (22) for the minimal (green), zero (blue), and maximal (red) possible correlation strength parameter γ. The inset shows a zoom. As one can see, especially in the inset, for the maximal value of $\gamma = \gamma_{\max}$, there exist threshold values, that intersect three times with $F(\kappa)$ and we therefore expect three nontrivial solutions κ. The dashed

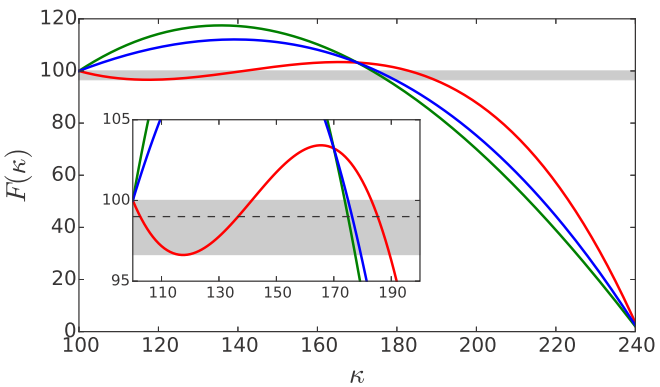

FIG. 6. The figure shows $F(\kappa)$ as function of the population degree κ for three different values of the correlation strength parameter γ. The green line corresponds to the minimal possible value $\gamma = \gamma_{\min} \approx -0.60 \times 10^{-6}$, the blue line to the uncorrelated case ($\gamma = 0$), and the red line to the maximal possible value $\gamma = \gamma_{\max} \approx 1.45 \times 10^{-6}$. The inset shows a zoom of the same graph, where the dashed black line shows an exemplary integer value for the threshold, here $\Theta = 99$, that intersects three times with $F(\kappa)$ for $\gamma = \gamma_{\max}$.

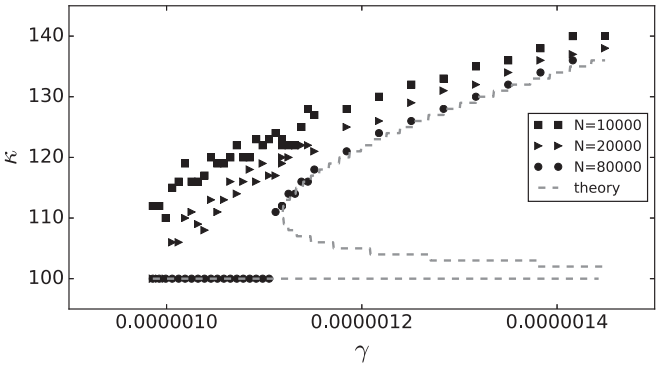

FIG. 7. Simulation results for correlated networks of different sizes at a threshold of $\Theta = 99$. A steady-state solution is shown as function of the correlation strength parameter. For this simulation, the initially active population degree was chosen to be $\kappa_0 = 150$.

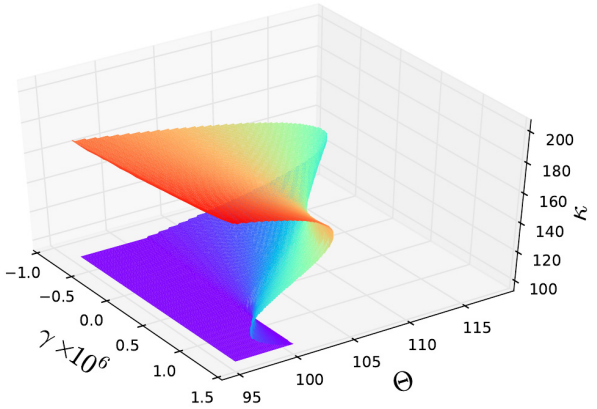

FIG. 8. The figure shows the solutions κ of the equation $0 = F(\kappa,\gamma) - \Theta$ within the maximally possible range of γ for networks with flat degree distribution in the range $100 \leqslant k \leqslant 240$. The color code simply indicates the height of the surface.

black line in the inset exemplarily shows the threshold $\Theta = 99$, which exhibits the property of more than two intersections with $F(\kappa)$ for $\gamma = \gamma_{\max}$. The corresponding joint distribution function $N(k,k')$ is shown in Fig. 1 in red, compared to the uncorrelated joint distribution function in blue. Figure 7 shows stable fixed points of the system as function of the correlation strength parameter γ for different network sizes at a threshold of $\Theta = 99$. Simulation results are indicated by blue, green and black marks (different colors represent different network sizes). Theoretically predicted results are indicated by the gray dashed line. For the simulations, each system was initialized at $\kappa_0 = 150$. The marks show steady state solutions of the system. They were approximated as discussed in Sec IV A for uncorrelated networks. One can see, that for the largest chosen system size of $N = 80\,000$ neurons, the expected and simulated results agree very well. For the smaller system sizes, the simulation results differ from the expected. Especially at the point where the second unstable solution emerges, the discontinuous "jump" is only observed for the larger system sizes. Unstable fixed points for this situation were also recovered from direct simulations (not shown). In Fig. 8 we show a surface of solutions of the self-consistent equation $0 = F(\kappa,\gamma) - \Theta$ for the entire possible range of the strength parameter γ. One can see that for smaller values of γ, there are two nontrivial solutions κ, while for large correlation strength parameters, four κ's can be found.

V. DISCUSSION

In Fig. 8, the lowest κ values correspond to a stable solution of the system, i.e., represent points, to which the system converges, depending on the initial conditions. The largest κ value displayed by this surface are unstable solutions. In the vicinity of that point, a slight change of initial conditions leads to the convergence of the system to a different stable point. Going above this value leads to vanishing activity in the system, i.e., to $\kappa = 0$, which is always a stable fixed point. For higher correlation strength parameters γ, one additional stable and one additional unstable fixed point emerge. However, this is only possible for threshold values below the minimal population degree. One of the stable fixed points is then $\kappa_s = 100$, which means that all populations are completely active.

Note that Fig. 5 corresponds to a cut through the surface displayed in Fig. 8 in the Θ-κ plane at $\gamma = 0$. Figure 7, on the other hand, corresponds to a cut in the γ-κ plane at $\Theta = 99$. Approaching the vertex in the former can be done quite precisely, as the correlation strength parameter can be arbitrarily chosen. In the latter case, this is not possible, because only integer values of Θ are allowed here. (Note that the surface shown in Fig. 8 was also calculated for noninteger numbers of Θ, which we do not allow in our simulations at this point.)

Our simulations recover the theoretically predicted values quite precisely for system sizes that are appropriately large. For too small system sizes, the simulation results differ more and more from the theoretical predictions. For example, for uncorrelated network with degree range $k \in [100,240]$, the vertex of $F(\kappa)$ lies very closely and actually slightly above $\Theta = 112$ and accordingly we would expect a steady-state solution for that threshold, which we, however, do not find for a network consisting of $N = 80\,000$ neurons. The simulation of that particular situation is displayed in Fig. 9. As one can see, there is a regime of initially active neurons, which change only very little in a range of roughly 20–80 iteration steps. However, iterating further eventually leads to vanishing number of active neurons for all initial conditions. Thus, we find no nonzero

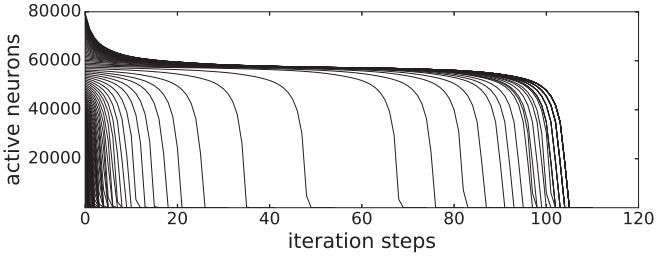

FIG. 9. The figure above shows the number of active neurons as function of iteration steps for an uncorrelated network with different initial conditions, similar to Fig 3, but at a threshold of $\Theta = 112$.

steady state solution for $\Theta = 112$. This could probably be circumvented by going to even larger system size, but also doesn't really provide any more insight. While it is known that networks of McCullogh-Pitts neurons can lead to bistability in the activity of the network [22], we showed how the structural properties of the network affect and even introduce these stable patterns.

A. Stability of the steady-state solutions of the system

Steady-state solutions for our system of interest are defined by

$$\dot{u}_k = 0, \tag{35}$$

with

$$\dot{u}_k = -u_k + f\left(\sum_{k'} N(k,k')u_{k'}\right), \tag{36}$$

where u_k is the activity of population k. The function f introduced in Sec. II A is the recurrent input function of sigmoidal form (which will then be approximated by a Heaviside step function). For the fixed point we then get

$$u_k = \theta\left(\sum_{k'} N(k,k')u_{k'} - \Theta\right). \tag{37}$$

Discussing the stability of fixed points of this system in a general manner is problematic, because Eq. (37) fixes u_k to either 1 or 0. It is intuitive that there is a certain degree $k = \kappa$ that represents a step solution, i.e., $u_k = \theta(\kappa - k)$. Evidently, the degree κ satisfies the equation

$$F(\kappa) - \Theta = 0, \tag{38}$$

where we again introduced $F(\kappa) = \sum_{k'=\kappa}^{k_{\max}} N(\kappa,k')$.

Although the approximation in which u_k only takes two values, 0 or 1, together with the Heaviside recurrence function, is sufficient to reproduce the positions of the fixed points of dynamics, it is too rough to reasonably describe the temporal evolution of the system, and therefore to classify the stability properties of the fixed points. Let us consider a step-function distribution of $u_k = \theta(k - \kappa)$, and let us take κ_f to be the solution of $F(\kappa_f) - \Theta = 0$, where the argument of the recurrence function changes its sign. Let us consider the whole interval of k, $k_{\min} \leqslant k \leqslant k_{\max}$, and the values of u_k, which are $u_k = 0$ for $k < \kappa$ and $u_k = 1$ for $k \geqslant \kappa$. The whole interval of the k values can then be separated into subintervals where $u_k = \theta[F(\kappa) - \Theta]$, where $\dot{u}_k = 0$, and no changes take place, and the ones where $u_k \neq \theta[F(\kappa) - \Theta]$, where u_k change, namely grow or decay. This growth or decay initially takes place "vertically": all u_k in the corresponding domain grow or decay initially at the same rate, take values that are different from zero or unity, and during this growth or decay the assumption $u_k = \theta(\kappa - k)$ breaks down. A slight modification of the model, however, allows for making statements about the stability.

Let us return to Fig. 4 and consider the domain of the realistic "front," in which u_k is neither close to zero nor to unity (i.e., the growth domain of u_k which is depicted by a vertical wall, when passing to the θ-function approximation). Let us now assume u_k in this domain to grow or to decay. Growing

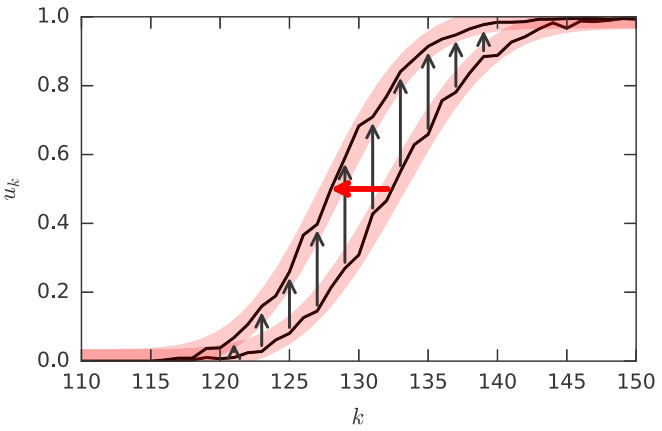

FIG. 10. The figure above shows the propagation of a population activity "front" from one exemplary iteration to the next. It can be seen, that a growing of u_κ in this domain leads to a shift of the front to the left (lower values of κ), as indicated by the red arrow. The red shaded lines show best fit error functions for each "front." Black arrows indicate the change in u_κ for exemplary values of κ.

of u_k then corresponds to the shift of the growth domain to the left, while decaying of u_k corresponds to shifting the domain to the right. Figure 4 gives a hint onto exactly this kind of "horizontal" behavior of the solution of the whole problem: The form of the front forms relatively early in the course of its temporal evolution, after which the spatial distribution of u_k keeps its form, but moves as a whole.

When going to the approximate, steplike form of the front, we now have to assume that this growing of u_k in the domain takes place by shifting the border between zero and unit values (the "front") to the left (to lower values of κ), while decaying corresponds to shifting this border to the right (larger values of κ). Shifting to the right takes place if $F(\kappa) - \Theta < 0$, and shifting to the left if $F(\kappa) - \Theta > 0$. Figure 10 illustrates this for two exemplary population activity "fronts." One corresponds to the other after exactly one iteration step. The direction of the front propagation is indicated by the red arrow, pointing from the median of the one front to the other. Black arrows show the evolution of u_κ for exemplary κ values before and after this one iteration step. The red shaded lines show fitted error functions. It can be seen that both "fronts" are well approximated by the error function and that the shape changes only very little in the course of one iteration.

Now we neglect the discreteness of k and consider the changes in some formal timelike variable τ, so that

$$\frac{d\kappa}{d\tau} = -[F(\kappa) - \Theta], \tag{39}$$

which depicts our discussion about the direction of the front's motion. Now we simply can discuss the stability of the front position using the standard method. The fixed-point front position κ_f is stable if

$$\left.\frac{dF(\kappa)}{d\kappa}\right|_{\kappa=\kappa_f} > 0 \tag{40}$$

(the "force" acting on the front is a restoring one) and unstable otherwise. For an uncorrelated network with $F(\kappa)$ given by Eq. (28) the nontrivial fixed point at a smaller value of κ is

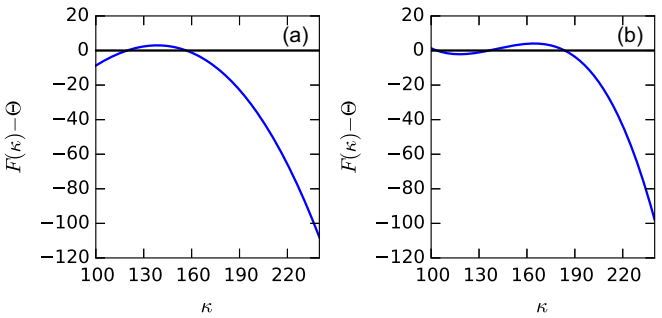

FIG. 11. The figure above shows a summary of the two possible cases for the stability discussion. (a) $F(\kappa)-\Theta$ for an uncorrelated network with flat degree distribution as discussed in Sec. IV A, with $\Theta = 108$, corresponding to Fig. 2. (b) The same for the maximally correlated case as discussed in Sec. IV B and for $\Theta = 99$, corresponding to the red line in Fig. 6. In both figures, the fixed points are defined by the intersection, and their stability by Eq. (40), i.e., the slope of $F(\kappa)$ at the intersection. Hence, the uncorrelated network with flat degree distribution gives rise to one stable and one unstable nontrivial fixed point. Degree correlations in networks with flat degree distribution can lead to a third nontrivial fixed point, which is here unstable.

therefore stable, and the one at the larger value is unstable. For the correlated network of our other example the situation is similar. A comparison of two exemplary cases is shown in Fig. (11). This is in agreement with what we see in our simulations.

On a final remark, we want to point out that the discrete time version of our system with step function θ as a transfer function [Eq. (30)] is very similar to the Hopfield model [23], which has been extensively studied in the context of storing patterns in neuronal networks and spin glasses, etc. This model is know to be able to exhibit cyclic or chaotic behavior if the interaction matrix, i.e., the adjacency matrix of the network, is not symmetric [24]. While this is generally the case for any directed network, our analytical considerations as well as the simulation results gave no hints onto cyclic or chaotic behavior for the networks studied in this work.

VI. SUMMARY AND OUTLOOK

In this work we formulated a description of steady activity states in complex networks and advertise that population statistics is sufficient to describe dynamics of this particular system. We have seen that approximating the population activity in neuronal networks by a function as simple as the Heaviside step function allows an analytical approximation for flat degree distributions, that is well retrievable by numerical simulations of binary neurons.

Throughout this study, we have only focused on the case of flat degree distributions, as those are easy to solve analytically. However, the presented formalism should hold for degree distributions that do not show a simple analytical approximation of κ.

ACKNOWLEDGMENTS

This work was supported by the Deutsche Forschungsgemeinschaft within the Project No. IRTG 1740.

APPENDIX A

1. Population equations

The population equations used in the text are the mean-field equations. As often, they may represent an uncontrolled approximation of the initial model based on interchanging averaging with a nonlinear operation, and may be obtained as a special limiting case of an exact theory in which the range of interaction (i.e., the total number of interacting sites) goes to infinity while the interaction strength goes to zero. In what follows we show that this is exactly what is done. As always, the accuracy of such approximation must be checked in explicit simulation, as it was done in the main text.

Let us return to our Eqs. (2) and (3) and note that the second term in the right-hand side of Eq. (3),

$$\tilde{f}(u_k) = \frac{1}{N_k} \sum_{i:k_i=k} f\left(\sum_j a_{ij} v_j\right) \tag{A1}$$

(assumed in the approximation to be a function of u_k), is the arithmetic mean of the recurrence functions f for the neurons of the k population in a given realization of the network. The number of k neurons in the network is usually large; in the limit of an infinitely large network Eq. (A1) defines the true statistical mean (mathematical expectation) of the recurrence function f for a k neuron. The approximation done in the population model corresponds to the approximation of the mean value of the function by the function of the mean value of its argument.

The aim of our discussion is to clarify what additional assumptions have to be done on the way, i.e., what kind of the limiting transitions are done, and how the accuracy of the approximation may be estimated. In what follows we assume that for each k population the mean population value of the activity u_k and that lower moments of v_i within each population are well-defined.

If not only the number of neurons in the network, but also the number of synapses k per neuron is large enough (which in our case is guaranteed by using the relatively large lower cut-off $k_{\min}$), the total number of connections of a k neuron to k' ones is also large, and the relative fluctuations of this number are small. Moreover, separating the sum over j into contributions of populations corresponding to different k', with $N(k',k)$ contributions on the average, we see that

$$\sum_j a_{ij} v_j \simeq \sum_{k'=k_{\min}}^{k_{\max}} N(k,k') u_{k'}. \tag{A2}$$

Using this expression in the argument of f [Eq. (A1)], we see that $\tilde{f}(u_k) = f[\sum_{k'} N(k,k') u_{k'}]$, which leads to our Eq. (4). Let us first rewrite the sum in the argument of f, $A_i = \sum_j a_{ij} v_j$ by first summing over all the neurons in the k' population connected to i, and then over all the k' populations,

$$A_i = \sum_j a_{ij} v_j = \sum_{k'=k_{\min}}^{k_{\max}} \sum_{j:k_j=k'} v_j^{(i)}.$$

Here, we introduced the notation $v_j^{(i)} = a_{ij}v_j$, where superscript (i) denotes the number of the neuron whose connections are considered. Further introducing $n_{k'}^{(i)} = \sum_{j:k_j=k'} a_{ij}$, i.e., the number of k'-neurons connected to neuron i, we rewrite this expression as

$$A_i = \sum_{k'=k_{\min}}^{k_{\max}} n_{k'}^{(i)} \sum_{j:k_j=k'} \frac{v_j^{(i)}}{n_{k'}^{(i)}}.$$

The second sum is the arithmetic mean of $v_j^{(i)}$ in the subpopulation of the k' population, namely for all k' neurons connected to i. According to the law of large numbers, for $n_{k'}^{(i)} \to \infty$ this sum tends to the mathematical expectation of v_j in the k' population, i.e., to $u_{k'}$, and its fluctuations between realizations of neighbors of i decay as $1/\sqrt{n_{k'}^{(i)}}$, so that this one tends to a deterministic limit which ceases to depend on the number i of the neuron considered. Thus,

$$\sum_{j:k_j=k'} \frac{v_j^{(i)}}{n_{k'}^{(i)}} = u_{k'} + \delta u_{k'} \simeq u_{k'} + \delta v_{k'}/\sqrt{n_{k'}^{(i)}},$$

where $\delta v_{k'}$ is the random fluctuation of the values of $v_{k'}$. Its typical size is given by the dispersion of the values of v_i within the k' population. In our model v_i represents normalized activities of individual neurons and is therefore limited to the range from 0 to 1, which also holds for means $u_{k'}$. Assuming that the neurons connected to the one under consideration are chosen randomly from the corresponding population, the dispersion is $\sigma_{k'}^2 = \langle u_{k'}^2 \rangle - \langle u_{k'} \rangle^2 < 1$. Summarizing, we see that Eq. (A1) turns to

$$\tilde{f}(u_k) \simeq \frac{1}{N_k} \sum_{i:k_i=k} f\left[\sum_{k'=k_{\min}}^{k_{\max}} n_{k'}^{(i)} \left(u_{k'} + \delta v_{k'}/\sqrt{n_{k'}^{(i)}} \right) \right].$$

Now we introduce the joint distribution function, i.e., the average number of links from the k' population to the k population, which is mean of $n_{k'}^{(i)}$ for all neurons i in the k population, i.e.,

$$N(k,k') = \frac{1}{N_k} \sum_{i:k_i=k} n_{k'}^{(i)}.$$

In the models like the ones discussed above, where the links are added to the node in a kind of a random process, the fluctuations δ_n of $n_{k'}^{(i)}$ around their means $N(k,k')$ are Poissonian and of the order of $\sqrt{N(k,k')}$, which gives us the possibility to calculate the expectation of the argument of f in Eq. (A1) to be

$$A_{i:k_i=k} = \sum_{k'=k_{\min}}^{k_{\max}} N(k,k') u_{k'}.$$

The fluctuations around this mean are given by

$$\delta A = \sum_{k'=k_{\min}}^{k_{\max}} N(k,k') \delta u_k' + \delta_n u_k$$

and are of the order of $\sqrt{N(k,k')}$ (the corresponding dispersion is $\sigma_A^2 \simeq aN(k,k')$ with the prefactor $a \leqslant 2$).

We note that the estimates above hold essentially for any transfer function f bounded on $[0,1]$, and what may change are only the prefactors in the correction terms $O(k_0^{1/2})$. In any model with initial activities distributed on $[0,1]$ they will stay bounded to the same interval during the whole temporal evolution of the system, and the estimates of the corresponding dispersions stay true. The step function discussed in the main text represents to some extent the worst case, and the bounds for twice differentiable functions f may be pushed tighter.

Let us now discuss what limiting transitions have to be done to make the approximation exact. First, as we have seen, the transition $k \to \infty$ has to be done. This can be done by rescaling of $P(k)$ in which the form of the distribution stays constant, but both $k_{\min}$ and $k_{\max}$ tend to infinity. For $N(k,k')$ we then obtain that this can be rewritten as a function of the relative link numbers $\nu = k/k_0$, and $\nu' = k'/k_0$ depending on the two dimensionless parameters, the correlation strength γ and the relative width $w = k_0 C^{-1}$: $N(k,k') = k_0 N(\nu,\nu';\gamma,w)$. In this notation for $k_0 \to \infty$, we will get

$$A_i \simeq k_0 u_k + O\left(k_0^{1/2}\right),$$

where the second contribution denotes the fluctuating part of the argument. This argument A of the f function [Eq. (A1)], however, diverges in the limit $k_0 \to \infty$ which limit thus does not exist in the mathematical sense. This is the typical situation in all mean-field approaches, where the interactions have to involve many particles (to create the mean field with negligible fluctuations) but the strength of this field does not have to diverge, exactly the same, as, say in an Ising model with long-range interactions, as discussed in Sec. 6.6 of Ref. [25]. This difficulty is overcome by explicitly introducing the coupling strength $c \propto k_0^{-1}$ and taking the argument of the transfer function to be $A_i = c \sum_j a_{ij} v_j$. In this case, the growth of the number of inputs of the neurons, leading to the decay of relative fluctuations but to the growth of the total impact, is compensated by the fact that the impact of each particular neuron gets smaller. Under the limiting transition $k_0 \to \infty$, the argument of the f function gets to be

$$A = u_k + O\left(k_0^{-1/2}\right),$$

so that fluctuations can be made arbitrarily small, and Eq. (4) gets exact. We note that for a step function $f(x) = \theta(x - \Theta)$ such a renormalization of $x \to cx$ is equivalent to the rescaling of Θ according to $\Theta' \to c^{-1}\Theta = k_0\Theta$, as it follows from the property $\theta(cx) = \theta(x)$ for any $c > 0$. This gives us a simpler recipe for rescaling: The theory gets exact in a limit when $k_0 \to \infty$ provided the value of Θ is rescaled accordingly. The behaviors of the systems with the same $k_{\min}/k_0, k_{\max}/k_0$, and Θ/k_0 will be similar.

For a flat and relatively narrow distribution $N(k,k') \simeq N(k,k) \simeq k_0$ the fluctuations of each term are of the order of $\sqrt{k_0}$, i.e., by the order of $k_0^{-1/2}$ smaller than the mean, with approximately Gaussian distribution following by virtue of the Central Limit Theorem. This Gaussian distribution then translates into the error function used for the fit of the actual distribution of activities for a Heaviside-θ recurrence function

f used, e.g., in Fig. 10 and also for the gray shaded front form in Fig. 4, since

$$\tilde{f}(u_k) = \frac{1}{N_k}\sum_{i=1}^{N_k} f(A_i) \simeq \left\langle \theta(A_{i:k_i=k} - \Theta) \right\rangle = F(A),$$

where $F(A)$ is the cumulative distribution function of the distribution of $A_{i:k_i=k}$. For the Gaussian distribution of $A_{i:k_i=k}$ it is related to the error function. The widths of the fronts obtained in simulations indeed are error-function-like, and their widths are indeed of the order of $\sqrt{k_0}$.

2. Constraints on the joint distribution function

Equation (9) follows from the positivity of probability. Equation (10) holds because of normalization $\sum_{k'} P(k'|k) = 1$ or $\sum_{k'} P(k,k') = P_e(k)$. For undirected networks, Eq. (11) can be seen by writing out the equation with the definition of the joint distribution function Eq. (7) and using the detailed balance condition

$$\sum_k k P(k) P(k'|k) = \sum_k k' P(k') P(k|k') \tag{A3}$$

$$= k' P(k') \sum_k P(k|k') \tag{A4}$$

$$= k' P(k'). \tag{A5}$$

For directed networks, the joint probability density $P(k,k')$ is not generally symmetric and accordingly detailed balance doesn't hold. However, from the constraint of a given degree distribution AND equal in and out degree, it follows that the summation of the joint degree distribution over either degree must yield the edge degree distribution of the remaining degree (compare to Eq. (17) in Ref. [15]). That is,

$$\sum_k P(k,k') = P_e(k) \quad \text{and} \quad \sum_{k'} P(k,k') = P_e(k'). \tag{A6}$$

Then again, from the normalization of the conditional probability $\sum_k P_e(k) g(k,k') = 1$ we find

$$\sum_k k P(k) P(k'|k) = \sum_k \frac{k P(k) P(k,k')}{P_e(k)} \tag{A7}$$

$$= \sum_k \frac{k P(k) P_e(k) P_e(k') g(k,k')}{P_e(k)} \tag{A8}$$

$$= P_e(k') \sum_k k P(k) g(k,k') \tag{A9}$$

$$= \langle k \rangle P_e(k') \sum_k P_e(k) g(k,k') \tag{A10}$$

$$= \langle k \rangle P_e(k') \tag{A11}$$

$$= k' P(k'). \tag{A12}$$

3. General form of the joint distribution function

Equation (13) is obviously fulfilled, if η is of the form

$$\eta(k,k') = g(k) h(k'), \qquad \text{with} \tag{A13}$$

$$\sum_{k=k_{\min}}^{k_{\max}} g(k) = 0 \quad \text{and} \quad \sum_{k'=k_{\min}}^{k_{\max}} h(k') = 0. \tag{A14}$$

These conditions are satisfied, if g,h are of the form

$$\phi(k) = \tilde{\phi}(k) - \frac{1}{dk}\sum_{k=k_{\min}}^{k_{\max}} \tilde{\phi}(k), \tag{A15}$$

where $dk = k_{\max} + 1 - k_{\min}$. For a first discussion we choose $g(k) = \phi(k)$, $h(k') = \phi(k')$ and $\tilde{\phi}(k) = k$, so that

$$\phi(k) = k - \frac{1}{dk}\sum_{k=k_{\min}}^{k_{\max}} k = k - k_0, \tag{A16}$$

where $k_0 = (k_{\max} + k_{\min})/2$, which correspondingly leads to Eq. (15).

APPENDIX B

In the present study, we focused on the steady-state solutions for the population activity in recurrent neuronal networks, which are analytically solvable as, for example, in the case of flat degree distributions. In this Appendix, we proceed to show that the population equations derived still perform well for degree distributions different from flat ones, for time continuous situations, and for transfer functions different from step functions. We also note that the population equations work well for networks of leaky integrate and fire neurons as considered in Ref. [10]. The discussion below is not a general proof of the concepts discussed, but it illustrates the usefulness of the approach for situations different from the simplest one considered above.

1. Steady-state firing in networks with other degree distributions

While in general the function $F(\kappa)$, Eq. (22), might not be evaluated analytically, it can always be calculated numerically for a given network. We start by studying an Erdos-Renyi (ER) random graph [26] of similar size and mean degree as the networks studied before, i.e., the one with $N = 100\,000$ and $\langle k \rangle = 200$. For the network creation we used the igraph software package for complex network research [27]. Figure 12 shows the joint degree distribution $N(k,k')$, "measured" from the obtained network (in blue), compared to the corresponding distribution calculated according to Eq. (8) for an uncorrelated random network with a binomial degree distribution $P(k) = \binom{N-1}{k} p^k (1-p)^{N-1-k}$ with p denoting the probability that any two nodes share a link. For better visibility, only every fourth degree displayed in the plot. In this example, the value $p = 0.001$ was used both for the creation of the network and for the calculation of the joint degree distribution. The measured and the calculated joint degree distributions agree reasonably well for intermediate values of k, while there are large deviations towards the smallest and largest measured values of k. This echoes bad statistics, which is caused by the very few actual nodes of these extreme degrees. (In this particular example, the correct stable steady-state solution is calculated for population degrees above $k = 153$. The total number of neurons of all populations including and below this degree was 21 of 100 000.) Figure 13 shows a summary of the simulation results for the ER graph. The two top panels, Figs. 13(a) and 13(b), show the number of

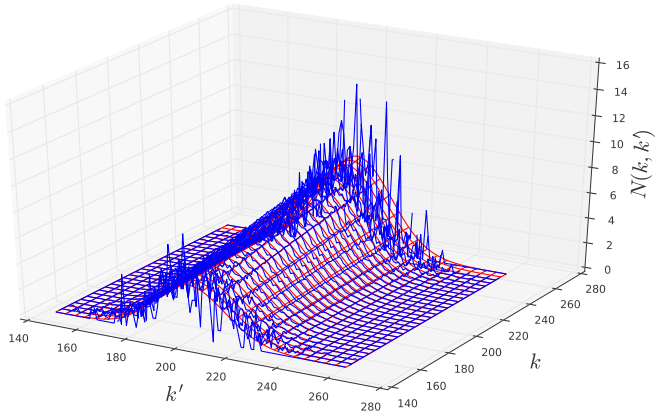

FIG. 12. The figure above shows the joint distribution function, calculated from a realization of a random graph as described in the text (in blue), compared to the joint distribution function calculated from Eq. (8) (in red). In that case, the degree distribution is given by a binomial distribution. It can be seen that the two surfaces differ significantly toward the maximum and minimum in-degree k.

active neurons and the population activity u_k after subsequent iteration steps for two different initial conditions. Red and blue lines correspond to an initially active population degree slightly below ($k_{\text{init}} = 185$) and slightly above ($k_{\text{init}} = 186$) the unstable fixed point, respectively. The result for the lower initial population degree converges to a stable steady state of active neurons, the other one leads to vanishing activity, similar to the behavior described in the sections above. The lower panel of Fig. 13 shows the stable (red dots) and unstable (blue hollow dots) fixed point of the system as function of the neuron threshold Θ, compared to the expected result from Eq. (23), shown by the black solid and dashed lines for $N(k,k')$ calculated and $N(k,k')$ "measured." It can be seen that the simulation results agree very well with the expected result for the most part, with the exception of results for stable fixed point for low thresholds Θ. This deviation is caused by the bad statistics due to the very few, if any, nodes at those extreme degrees. The results show that the method described is not limited to a particular flat degree distribution, but can also be applied for the investigation of biologically more relevant situations.

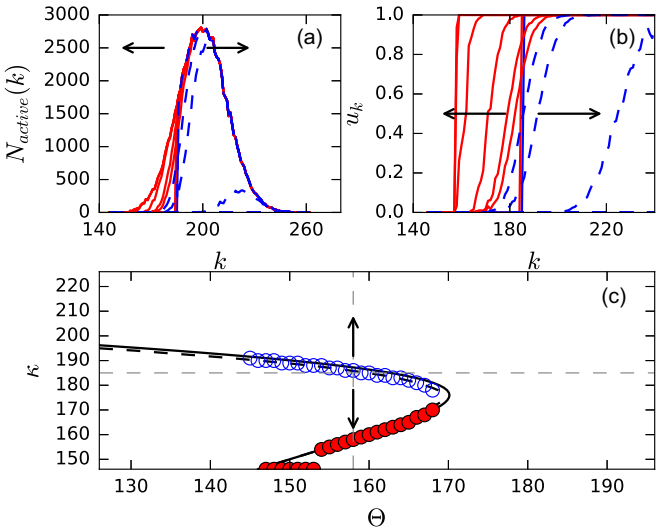

FIG. 13. (a) The active neurons, sorted by degree and (b) the corresponding population activity. The system was initialized slightly above (blue dashed lines) and slightly below (red lines) the critical population degree and then iterated, until the steady state was reached (cf. Fig. 4). (c) The stable (red dots) and unstable (blue hollow dots) solutions of the system, compared to the expected result.

2. Temporal evolution

Let us now present results of numerical simulations for an exemplary sigmoidal transfer function f different from the step function. We note that in this case the continuous-time approach is more appropriate. We therefore assume that the (normalized) activity v_i of every individual neuron can take continuous values between 0 and 1, and integrate the system of Eqs. (1) using a simple forward Euler scheme:

$$v_i(t+dt) = v_i(t) + \frac{dt}{\tau}\left[-v_i(t) + f\left(\sum_j a_{ij} v_j - \Theta\right)\right]. \tag{B1}$$

Note that the map described by Eq. (30) is equivalent to Eq. (B1) if we choose the time step to be equal to the time scale τ, and both equal to unity, $dt = \tau = 1$, and take f to be a θ function. The macroscopic simulations are equivalently performed using a forward Euler integration scheme for the population equations, Eq. (4):

$$u_k(t+dt) = u_k(t) + \frac{dt}{\tau}[-u_k(t) + f\left(\sum_{k'} N(k,k') u_{k'} - \Theta\right)]. \tag{B2}$$

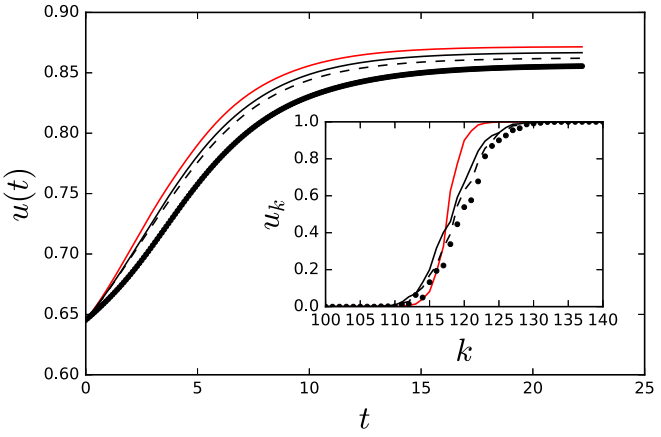

FIG. 14. The figure above shows the temporal evolution of the relative activity of recurrent neuronal networks of different sizes (microscopic simulation, black lines), compared to the evolution of the relative activity as expected from the population equation, Eq. (4) (macroscopic simulation, red line). The black dotted, dashed, solid lines correspond to network sizes of $N = 14\,100$, $N = 28\,200$, and $N = 84\,600$, respectively, 100, 200, 600 neurons per population. The inset shows the population activity u_k, as function of the degree k with the same color code.

In this section, we return to the flat degree distribution and display simulation results comparing the temporal evolution of the relative activity of the networks as given by direct simulations and by the population equations. The relative activity is defined as

$$u(t) = \frac{1}{k_{\max} + 1 - k_{\min}} \sum_k u_k(t) = \frac{1}{N} \sum_i v_i(t). \tag{B3}$$

Figure 14 shows a comparison between microscopic simulation results and ones of the macroscopic description of the temporal evolution of the relative activity for a recurrent neuronal network with a flat degree distribution within $k \in [100,240]$ for different network sizes. The inset shows the normalized population activity u_k attained after the steady state was reached for the macroscopic simulation [Eq. (B2)] (in red) and for the microscopic simulation in [Eq. (B1)] (in black). For all simulations the time scale τ was set to unity, and the integration time step was taken to be $dt = 0.1$ (smaller time steps did not change the results in any significant way). The steady state was identified when two consecutive relative activity values differed by less then 1%. We used the transfer function $f(x) = 1/[1 + \exp(-x + 108)]$ for both the microscopic and the macroscopic simulation. The value 108 can be associated with the threshold degree Θ for a step transfer function $f(x) = \theta(x - \Theta)$. The systems where initialized so that $u_k = 1$ for $k \geqslant 150$ and $u_k = 0$, otherwise. Note that for this particular choice of the transfer function and degree distribution no simple steady-state solution in form of a step above (below) which all neurons are active (inactive) arises. However, the population Eqs. (4) still give a good approximation for the activity of the neuronal populations. The quality of the approximation improves for larger system sizes, as expected, and this holds both for the temporal evolution of the relative activity and for the resulting shape of the dependence of the population activity on the degree k.

[1] A. Pouget, P. Dayan, and R. Zemel, Nat. Rev. Neurosci. **1**, 125 (2000).
[2] B. B. Averbeck, P. E. Latham, and A. Pouget, Nat. Rev. Neurosci. **7**, 358 (2006).
[3] L. Yassin, B. L. Benedetti, J.-S. Jouhanneau, J. A. Wen, J. F. Poulet, and A. L. Barth, Neuron **68**, 1043 (2010).
[4] S. Nigam, M. Shimono, S. Ito, F.-C. Yeh, N. Timme, M. Myroshnychenko, C. C. Lapish, Z. Tosi, P. Hottowy, W. C. Smith *et al.*, J. Neorosci. **36**, 670 (2016).
[5] C. Lee, W. H. Rohrer, and D. L. Sparks, Nature **332**, 357 (1988).
[6] A. P. Georgopoulos, A. B. Schwartz, R. E. Kettner *et al.*, Science **233**, 1416 (1986).
[7] W. Singer, Neuron **24**, 49 (1999).
[8] I. Dean, N. S. Harper, and D. McAlpine, Nat. Neurosci. **8**, 1684 (2005).
[9] N. Brunel and J.-P. Nadal, Neural Comput. **10**, 1731 (1998).
[10] C. Schmeltzer, A. H. Kihara, I. M. Sokolov, and S. Rüdiger, PloS one **10**, e0121794 (2015).
[11] H. S. Seung and H. Sompolinsky, Proc. Natl. Acad. Sci. U.S.A. **90**, 10749 (1993).
[12] M. Shamir and H. Sompolinsky, Neural Comput. **18**, 1951 (2006).
[13] M. I. Chelaru and V. Dragoi, Proc. Natl. Acad. Sci. U.S.A. **105**, 16344 (2008).
[14] E. D. Adrian, J. Physiol. **61**, 49 (1926).
[15] S. Weber and M. Porto, Phys. Rev. E **76**, 046111 (2007).
[16] S. Johnson, J. J. Torres, J. Marro, and M. A. Munoz, Phys. Rev. Lett. **104**, 108702 (2010).
[17] W. S. McCulloch and W. Pitts, Biometrics **4**, 91 (1948).
[18] R. Xulvi-Brunet and I. M. Sokolov, Acta Phys. Pol. B **36**, 1431 (2005).
[19] G. B. Ermentrout and D. H. Terman, *Mathematical Foundations of Neuroscience*, Vol. 35 (Springer Science & Business Media, Berlin, 2010).
[20] G. Palm and F. Sommer, Network: Comput. Neural Syst. **3**, 177 (1992).
[21] W. M. Kistler and C. I. De Zeeuw, Neural Comput. **14**, 2597 (2002).
[22] W. Gerstner and W. M. Kistler, *Spiking Neuron Models: Single Neurons, Populations, Plasticity* (Cambridge University Press, Cambridge, 2002).
[23] J. J. Hopfield, Proc. Natl. Acad. Sci. U.S.A. **81**, 3088 (1984).
[24] D. J. MacKay, *Information Theory, Inference and Learning Algorithms* (Cambridge University Press, Cambridge, 2003).
[25] J. J. Binney, N. J. Dowrick, A. J. Fisher, and M. Newman, *The Theory of Critical Phenomena: An Introduction to the Renormalization Group* (Oxford University Press, Oxford, 1992).
[26] P. Erdos and A. Rényi, Publ. Math. Inst. Hung. Acad. Sci. **5**, 17 (1960).
[27] G. Csardi and T. Nepusz, InterJournal **Complex Syst.**, 1695 (2006).